Edge-pumped passively Q-switched thin Nd:YAG slab lasers

Xiaojin Cheng (程小劲), Zhimin Wang (王志敏), Fan Chen (陈 凡), and Jianqiu Xu (徐剑秋)

Shanghai Institute of Optics and Fine Mechanics, Chinese Academy of Sciences, Shanghai 201800

Received November 6, 2007

We report a high-power thin Nd:YAG slab laser with slab dimension of $1 \times 10 \times 60$ (mm) partially edge-pumped by diode laser arrays. Passive Q-switching is achieved with a Cr^{4+}:YAG microchip adopted as the saturable absorber mirror. The pulse duration is around 10 ns while the pulse repetition rate is higher than 10 kHz. The average output power of 70 W is obtained with a slope efficiency of 36%. The diffraction limited beam quality in the thickness direction is obtained by controlling the pump beam diameter inside the slab. The laser head is very compact with size of only $60 \times 74 \times 150$ (mm).

OCIS codes: 140.3540, 140.3480, 230.7400.

Thermally induced distortion usually blocks the solid-state laser scaling to higher output power while maintaining good beam quality. Slab geometrical laser has been proven to be an effective design to reduce thermally induced stress and aberration. Various configurations have been proposed for slab lasers, e.g., zig-zag slab lasers[1−4], face pumped[5−7] and partially end-pumped slab lasers[8,9], and slab lasers with unstable resonators[2,10]. The stress fracture limit is inversely proportional to the thickness of slab crystal. Thin slab geometry is beneficial for high average power lasers. In some industrial applications, e.g., drilling, cutting, and material processing, pulsed lasers with high peak power and high repetition rate are desired. Compared with active Q-switching, passively Q-switched laser offers advantages of low-cost, reliability, and simplicity of operation and maintenance[11−13]. This paper reports a high-power passively Q-switched thin Nd:YAG slab laser. A Cr^{4+}:YAG microchip is adopted as saturable absorber mirror. Average output power of 70 W with a slope efficiency of 36% is obtained.

The experimental setup is depicted in Fig. 1, where the Nd:YAG crystal slab was $1 \times 10 \times 60$ (mm) and Nd^{3+} ion doping concentration is 1.0 at.-%. The slab was clamped by micro-channel heat sinks from two large surfaces. A 100-μm-thick indium foil was filled between the crystal slab and the heat sink in order to reduce the thermal and mounting stress. The temperature of cooling water was 20 °C. To minimize the mounting stress during assembly, mount of the slab on the heat sink was monitored by an interferometer. Aberrant fringes should be eliminated by adjusting the locking screws. The dimension of a finished laser head was about $60 \times 74 \times 150$ (mm).

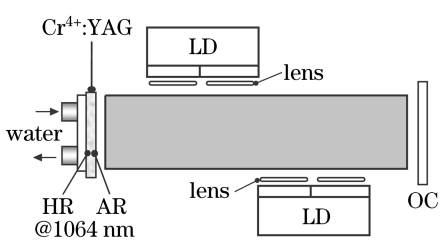

Fig. 1. Experimental setup of passively Q-switched thin Nd:YAG slab laser.

The laser was passively Q-switched by a Cr^{4+}:YAG micro-chip with size of $0.5 \times 5 \times 15$ (mm). One surface of the Cr^{4+}:YAG chip was high-reflectivity (HR) coated while another one was anti-reflectivity (AR) coated at 1064 nm. Thus, the Cr^{4+}:YAG micro-chip acted as a saturable absorber mirror in the slab laser. The initial transmission of the Cr^{4+}:YAG saturable absorber mirror was 90%. Since the slab laser was designed working in high power regime, the Cr^{4+}:YAG chip was force-cooled by a micro-channel heat sink attached to its back surface.

To acquire single mode oscillation in compact resonator, we controlled the pump beam diameter to match the fundamental laser mode inside the Nd:YAG slab. In such a way, higher-order modes would be filtered out due to lower gain outside the pump range. Calculated from $ABCD$ matrix method the laser beam radius was about 0.2 mm, so we designed the pump beam radius to be 0.25 mm and chose 1-mm-thick Nd:YAG slab. Two horizontal laser diode (LD) arrays, each consisting of three LD bars, closely pumped the slab from both edges. Micro cylindrical lens of 600 μm in diameter was employed to collimate the pump beam from the LD arrays. The emitted pump beam was about 0.5 mm ($1/e^2$) in diameter with the divergence angle of 2°. The pump beam from two edges was adjusted carefully to be in a same plane.

The distributions of temperature and stress in the slab were analyzed numerically to ensure the laser operating safely. The temperature difference in the thickness and width directions were 3 and 4 °C, respectively. The temperature gradient in the thickness direction was 3 °C/mm, which was about one order of magnitude higher than that of 0.4 °C/mm in the width direction. The thermal lens effects in the thickness direction is much larger than that in the thickness direction. The thermal stress component S_{xx} is two orders of magnitude higher than the thermal stress component S_{yy}. The maximum thermal stress component S_{xx} occurring at the arris of slab was 120 kg/cm^2 under 220-W pump power. It is much less than the fracture stress limit of Nd:YAG crystal, i.e., $1800 - 2100$ kg/cm^2[14]. The thin slab laser can bear more pump power than currently used.

The micro-channel heat sink was manufactured with channel's diameter of 0.5 mm, length of 55 mm, and pitch of 1.5 mm, respectively. The non-micro-channel

1671-7694/2008/050364-02

heat sink was made by drilling a single hole of 5-mm in diameter in a copper block. Figure 2 compares the focal length of the thermal lens when different heat sinks were used. Since heat removal with the micro-channel heat sink is more efficiently, the thermal focal length is longer. When using the non-micro-channel heat sink in the slab laser, the laser output power rolls back when the pump power reaches 110 W, revealing serious thermal distortion in the crystal slab.

To achieve higher repetition rate and higher output power, it needed high initial transition of the saturable absorber. We chose 90% of initial transition of the saturable absorber, and then the Cr^{4+} ions concentration was calculated from $N_{s0} = -\ln T/\sigma_g l_s$. The giant pulse occurs when the saturable absorber is saturated to transparent and the photon density reaches the maximum. From numerical calculations, we find that the repetition rate is higher than 10 kHz. The measured pulse sequences at 220-W pump power are shown in Fig. 3. The pulse duration is about 10 ns, resulting in the peak power of 0.7 MW. The peak power fluctuation from pulse to pulse is about 5%. The agreement between the calculation and experiment is very well.

Output power versus pump power with output coupling of 5%, 9%, 17% are compared in Fig. 4. The threshold of pump power was around 10 W. With the optimized output coupling of 9%, the maximum average power of 70 W was achieved with a slope efficiency of 36% when the pump power was 220 W. Output laser power grew linearly with increasing the pump power. The beam propagation factor M_y^2 in the thickness direction was 1.4, indicating near single-mode oscillation in the thickness direction. In the width direction, the beam profile was multi-mode due to the weakness of the plane-parallel resonator. If unstable resonator or graded reflectivity mirrors are adopted, good output beam quality in the width direction can be acquired.

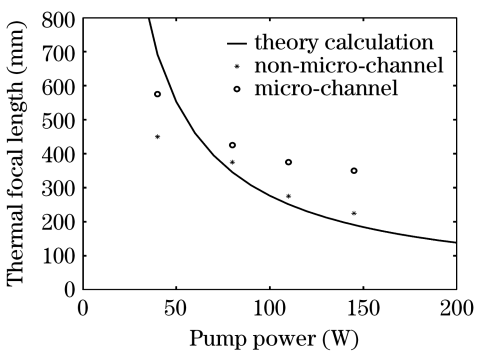

Fig. 2. Thermal focal length versus pump power.

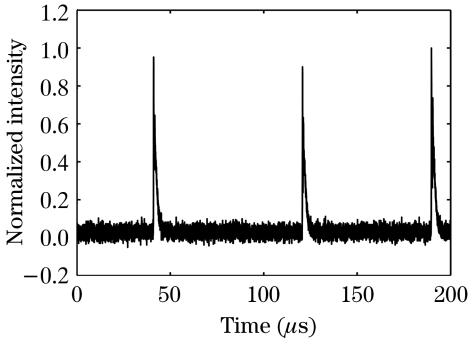

Fig. 3. Measured passively Q-switched laser pulse sequence.

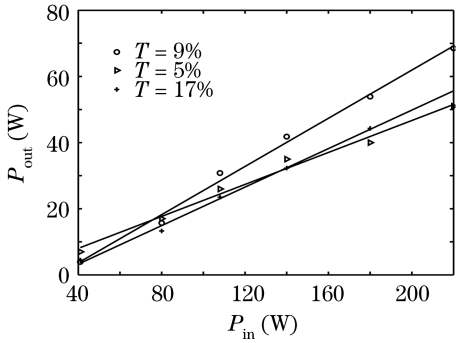

Fig. 4. Output laser power versus pump power.

In summary, high-power, high repetition rate thin Nd:YAGb slab laser was demonstrated. Output average power of 70 W with a slope efficiency of 36% was acquired when pump power was 220 W. The repetition rate higher than 10 kHz and the pulse width around 10 ns were demonstrated. Near diffraction limited beam quality in the thickness direction was obtained by precise control of the pump beam width inside the slab. An obvious advantage of this kind of lasers is their relatively compact design with the footprint less than 100 mm^3 and simple replacement of every part.

X. Cheng and Z. Wang contribute equally to this paper. This work was supported by the National Natural Science Foundation of China under Grant No. 60678016. X. Cheng's e-mail address is xjcheng@siom.ac.cn.

References

1. T. J. Kane, R. C. Eckardt, and R. L. Byer, IEEE J. Quantum Electron. **19,** 1351 (1983).
2. D. Mudge, P. J. Veitch, J. Munch, D. Ottaway, and M. W. Hamilton. IEEE J. Sel. Top. Quantum Electron. **3,** 19 (1997).
3. T. S. Rutherford, W. M. Tulloch, S. Sinha, and R. L. Byer, Opt. Lett. **26,** 986 (2001).
4. T. S. Rutherford, W. M. Tulloch, E. K. Gustafson, and R. L. Byer, IEEE J. Quantum Electron. **36,** 205 (2000).
5. A. Faulstich, H. J. Baker, and D. R. Hall, Opt. Lett. **21,** 594 (1996).
6. Jones, Jr. and B. William, "Face-pumped laser with diffraction-limited output beam" US patent 4,214,216 (July 22, 1980).
7. J. R. Lee, H. J. Baker, G. J. Friel, G. J. Hilton, and D. R. Hall, Opt. Lett. **27,** 524 (2002).
8. K. Du, N. Wu, J. Xu, J. Giesekus, P. Loosen, and R. Poprawe, Opt. Lett. **23,** 370 (1998).
9. P. Shi, D. Li, H. Zhang, Y. Wang, and K. Du, Opt. Commun. **229,** 349 (2004).
10. K. Yasui and Y. Takenaka, Appl. Opt. **40,** 3547 (2001).
11. G. Xiao and M. Bass, IEEE J. Quantum Electron. **33,** 41 (1997).
12. J. J. Degnan, IEEE J. Quantum Electron. **31,** 1890 (1995).
13. Z. Wang, X. Ye, T. Fang, and J. Xu, Opt. Rev. **12,** 391 (2005).
14. W. Koechner, *Solid-State Laser Engineering* (5th edn.) (Springer, Berlin, 1999).